



Ultrasonographic Characteristics of the Stifle Joint in Clinically Normal Donkeys (*Equus asinus*)

Marwa H Hassan* and Ahmed I Abdelgalil

Department of Surgery, Anesthesiology and Radiology, Faculty of veterinary medicine, Cairo University. PO Box 12211, Giza, Egypt

*Corresponding author: dr.marwa.hamdi2@gmail.com

Article History: 20-013 Received: January 14, 2020 Revised: February 07, 2020 Accepted: February 16, 2020

ABSTRACT

Stifle ultrasonography is a widely accepted diagnostic tool that has been used for diagnosing articular and peri-articular stifle injuries in horses. Limited information is available regarding the ultrasonographic appearance of the stifle joint in donkeys. The aim of the present study was to describe the normal ultrasonographic characteristics of the stifle joint in clinically normal donkeys. A descriptive study was done on 15 clinically normal donkeys (30 joints). Ultrasonographic examination was done in a systematic manner including both supra- and infra-patellar regions. The patella, patellar ligaments and tibial tuberosity were taken as palpable anatomical landmarks for localization of different stifle structures. A detailed description of the ultrasonographic appearance of the quadriceps muscle, supra-patellar pouch and femoropatellar joint was done through the supra-patellar approach. In infra-patellar approach, the patellar ligaments, medial and lateral femorotibial joints, collateral ligaments, menisci, origin of peroneous tertius and popliteal tendon were described. Standardized, repeatable and reliable images were achieved from both approaches. Ultrasonography provided a clinically useful tool for diagnosing donkeys with stifle joint disease.

Key words: Donkey, Equine, Joint, Stifle, Ultrasound.

INTRODUCTION

Stifle joint disease is an important cause of hind limb lameness in equine (Jeffcott and Kold, 1982; Sullins 2011; Trencart *et al.*, 2016). The large and complex nature of the joint represents a diagnostic challenge for the equine practitioner (Reardon and Lischer, 2008).

Ultrasonography of the stifle joint was firstly described in horses in 1990 (Penninck *et al.*, 1990). Since that time it has been used as a complementary diagnostic tool along with clinical, radiographic and arthroscopic examination to diagnose horses with stifle joint diseases (Cauvin *et al.*, 1996; Coudry and Denoix, 2005; Denoix and Lacombe, 1996; Dik, 1995; Gottlieb *et al.*, 2016; Martins *et al.*, 2006; Whitcomb, 2012). It is relatively inexpensive technique with the advantage of portability and real-time dynamic examination. It provides excellent visualization of the soft tissue details allowing evaluation of the articular capsule, articular cartilage, menisci, synovial fluid, subchondral bone, intra- and peri-articular ligaments (Beccati *et al.*, 2013; Beccati *et al.*, 2015; Martins *et al.*, 2006; Penninck *et al.*, 1990).

The normal ultrasonographic examination of the stifle joint has been previously described in the horse (Cauvin, 2014; Dik, 1995; Penninck *et al.*, 1990), cattle (Kofler,

1999); sheep (Macrae and Scott, 1999) and dog (Nayseh *et al.*, 2015). Reviewing the veterinary literatures, there was a paucity of reports describing the normal ultrasonographic appearance of the stifle joint in donkeys. The aim of the present study was to describe the normal ultrasonographic characteristics of the stifle joint and its associated structures in clinically normal donkeys (*Equus asinus*).

MATERIALS AND METHODS

Animals

The present study was carried out on 15 clinically healthy adult *Equus asinus* donkeys (9 males and 6 females), aged between 3 and 7 years old (mean \pm SD; 5.2 \pm 1.5 years), weighing 160 - 220 kg (mean \pm SD; 192 \pm 23) and were assessed to have a body condition score of 5 (moderate) or 6 (more than moderate) based on a nine-point score system for donkeys (20). These donkeys were admitted to the clinic of the Faculty of veterinary medicine, Cairo University for diseases unrelated to the musculoskeletal system. All Donkeys were clinically normal based on orthopedic (visual examination at rest and motion, palpation and flexion test) and radiographic examinations (dorsoplantar, lateral and oblique views) of

all joints. Owners were aware that their donkeys will be included in research purpose and signed a consent indicating their agreement. All study procedures were done in accordance to and approved by the Institutional Animal Care and Use Committee.

Study design

A descriptive study was done on the stifle region of both right and left limbs (30 joints). Joints were prepared for routine ultrasonographic examination then an acoustic coupling gel was applied. Scanning was performed using 10 MHz linear probe (EXAGO ECM Co., Angouleme, France) including both longitudinal and transverse scans during full weight-bearing.

Imaging technique

Ultrasonographic examination was performed in a systematic manner through supra- and infra- patellar approaches. The patella, patellar ligaments and tibial tuberosity were taken as palpable anatomical landmarks for localization of different structures.

The supra-patellar approach included examination of the quadriceps muscle, supra patellar pouch and the femoropatellar joint (FP) joint. The infra-patellar approach included examination of the patellar ligaments, femorotibial joint (FT), collateral ligaments and menisci. Scanning of the patellar ligaments started with the palpable middle patellar ligament (MiPL) followed by the medial patellar ligament (MPL) and the lateral patellar ligament (LPL) in both longitudinal and transverse scans. The medial and lateral compartments of the femorotibial joint (FT) were evaluated in both longitudinal and transverse scans. Finally, scanning of medial collateral ligament (MCL), medial meniscus (MM), lateral collateral ligament (LCL), lateral meniscus (LM), popliteal tendon and common origin of the peroneus tertius (PT)/long digital extensor (LDE) was done.

Detailed description of the ultrasonographic characteristics of the structures being visualized in each scan was done. Image resolution, depth and time gain compensation were fixed during examinations. All examinations were done by the same examiner; images were stored digitally and evaluated by all authors.

RESULTS

Supra-patellar approach

Ultrasonographic examination of the supra-patellar region was done by placement of the transducer just proximal to the patella where the quadriceps muscle, supra-patellar pouch and FP joint could be imaged.

In longitudinal scan, the quadriceps muscle appeared as a homogenous hypoechoic structure with the characteristic muscular pattern. A sharp clearly defined anechoic interface was seen between the quadriceps muscle and the proximal hyperechoic patellar surface representing the supra-patellar pouch (Fig. 1).

The FP joint was visualized by placing the transducer transversely just above the proximal surface of the patella with downward tilting 30-45°. The articular cartilage of the FP joint appeared as a thin, anechoic line covering the hyperechoic surface of the trochlear ridges. The joint capsule of the FP joint appeared as a hypoechoic

structure (Fig. 2). The medial articular cartilage of the FP joint appeared wider than that of the lateral one.

Infra-patellar approach

The patellar ligaments, medial and lateral compartments of the FT joint, collateral ligaments, menisci, origin of PT and popliteal tendon were seen.

The patellar ligaments were efficiently visualized in both transverse and longitudinal scans. In transverse scan, the transducer was placed 1 cm above the tibial tuberosity. This position allowed visualization of the three patellar ligaments. The patellar ligaments were identified as oval-shaped hyperechoic structures with multiple finely dispersed minute anechoic dots within the vicinity of the ligament (Fig. 3, 4 and 5). The MiPL appeared more echogenic than the lateral and medial ligaments.

In longitudinal scan, the transducer was placed above the palpable patellar ligaments where the characteristic regular linear pattern was seen. The ligaments appeared as homogenous hyperechoic structures with multiple faint anechoic lines within the vicinity of the ligaments (Fig. 3, 4 and 5).

The medial and lateral compartments of the FT joint were visualized in both longitudinal and transverse scans through the cranial aspect of the joint just proximal to the tibial tuberosity.

In the transverse scan, the articular cartilage of the FT compartments was seen as thin anechoic line covering the hyperechoic surface of the proximal tibia (Fig. 6). The joint capsule and the infra-patellar fat pad appeared as heterogenous echogenic structures. The joint capsule couldn't be differentiated from the surrounding infra-patellar fat pad.

In longitudinal scan, the medial FT compartment was visualized by applying the transducer just close to the MPL where the joint space appeared as anechoic space between the hyper echoic femoral surface and the hypoechoic medial meniscus. The lateral FT compartment was visualized by placing the transducer just lateral to the LPL where the joint appeared as thin anechoic articular cartilage extended between the hyperechoic surfaces of tibia and femur. The medial compartment was relatively wider than the lateral one.

The MCL was visualized by placing the transducer about 1 cm medial to the MPL. The ligament appeared as thick, flat homogenous echogenic structure with regular linear pattern. The MM appeared as triangular homogenous hypoechoic structure which could be visualized distal to the MCL in the same scan (Fig. 7).

The LCL was visualized by placing the transducer about 3 cm lateral to the LPL. It appeared as thin homogenous echogenic structure. The LM and the popliteal tendon were seen in the same scan. The LM was seen as homogenous hypoechoic triangular structure distal to the LCL and the popliteal tendon (Fig. 7). Abaxial bulging of the lateral meniscus was seen in 6 joints (20%). The popliteal tendon was visualized in 15 joints (50%) where it appeared as a thin echogenic band between the LCL and LM.

The combined origin of both PT and LDE tendon was easily imaged just close to the LPL. It appeared as a flat echogenic structure dorsal to the hyperechoic surface of tibia (Fig. 8).

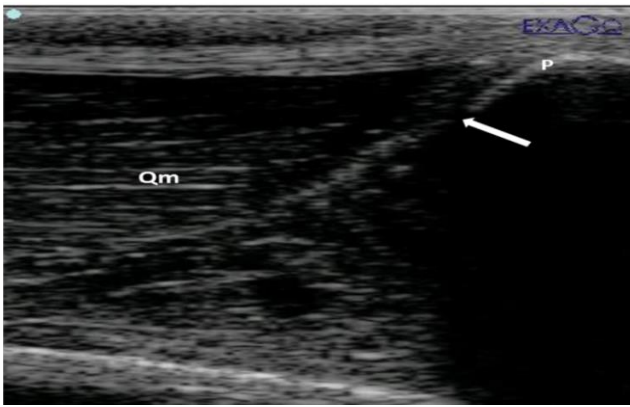


Fig. 1: Longitudinal scan at supra-patellar region demonstrating the quadriceps muscle (Qm) with its characteristic hypoechoic muscular pattern. The anechoic supra-patellar pouch (arrow) was seen between the hyperechoic patella (P) and the quadriceps muscle.

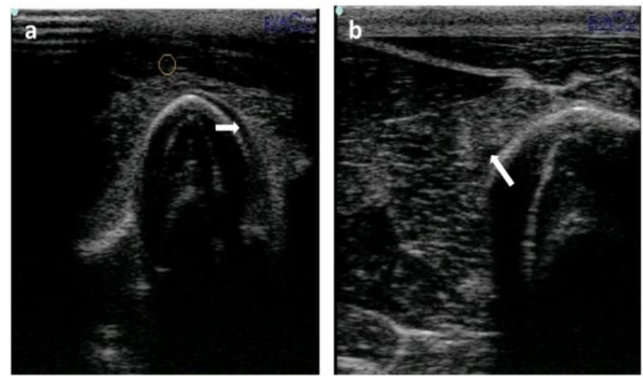


Fig. 2: Transverse scans of the medial (a) and lateral (b) compartments of the femoropatellar joint through supra-patellar approach. The articular cartilage was seen as a thin anechoic line (white arrows) covering the hyperechoic surface of the medial and lateral trochlear ridge.

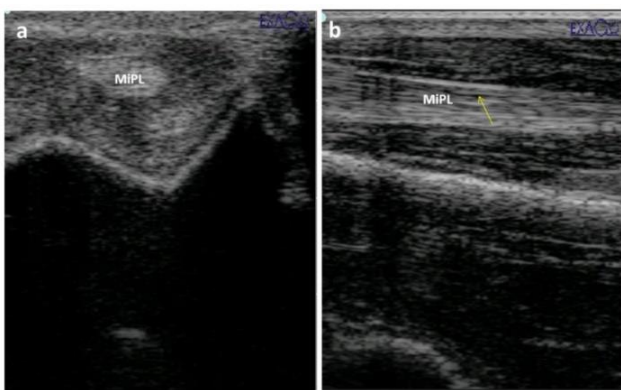


Fig. 3: Transverse (a) and longitudinal (b) scans of the middle patellar ligament (MiPL). The MiPL appeared as hyperechoic oval shaped structure surrounded with heterogeneously echogenic fat pad in transverse scan. In longitudinal scan, the MiPL was visualized as homogenous hyperechoic structure with characteristic regular linear pattern. Faint anechoic lines (arrow) were noticed within the vicinity of the ligaments.

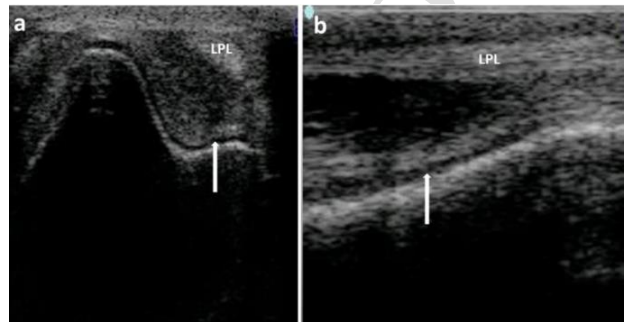


Fig. 4: Transverse (a) and longitudinal (b) scans of the lateral patellar ligament (LPL). The LPL appeared as flattened oval hyperechoic structure surrounded by heterogeneous hypoechoic fat pad in transverse scan. In longitudinal scan, LPL appeared as thin echogenic structure with characteristic regular linear pattern. Lateral articular cartilage of the femorotibial joint appeared as a thin anechoic line (arrow) covering the hyperechoic surface of the tibia.

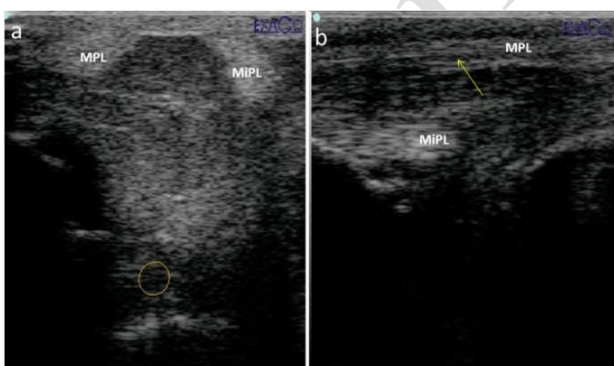


Fig. 5: Transverse (a) and longitudinal (b) scans of the medial patellar ligament (MPL). The MPL appeared as oval hyperechoic structure surrounded by heterogeneous hypoechoic fat pad. In longitudinal scan, MPL appeared as thin echogenic structure with characteristic regular linear pattern and fine anechoic lines (arrow) within the vicinity of the ligament. The MPL appeared less echogenic than the middle patellar ligament (MiPL).

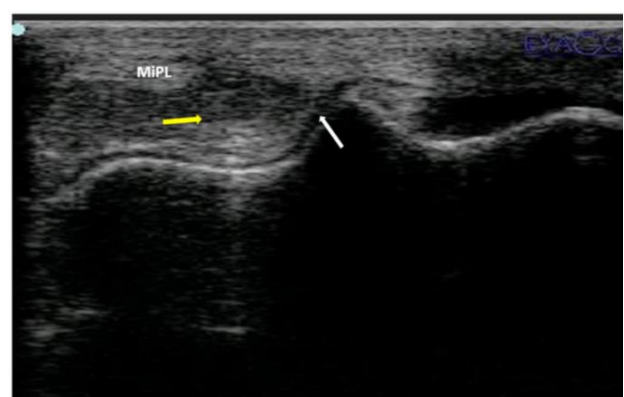


Fig. 6: Transverse scan of the femorotibial joint at proximal tibia demonstrating the characteristic thin anechoic articular cartilage (white arrows) imaged between the heterogeneously echogenic fat pad (yellow arrow) and the hyperechoic surface of the tibia.

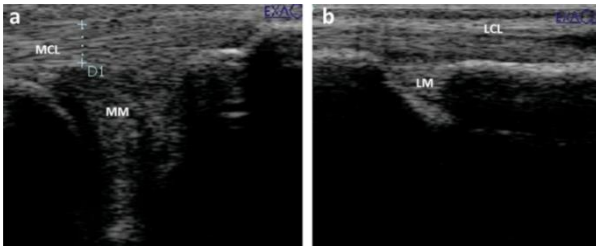


Fig. 7: Longitudinal scans of the medial collateral ligament (MCL) (a) and lateral collateral ligament (LCL) (b). The MCL appeared as a homogenous echogenic structure with linear pattern overlying the homogenous hypoechoic triangular structure of the medial meniscus (MM). The LCL appeared as thin echogenic structure overlying the homogenous echogenic triangular structure of the lateral meniscus (LM).

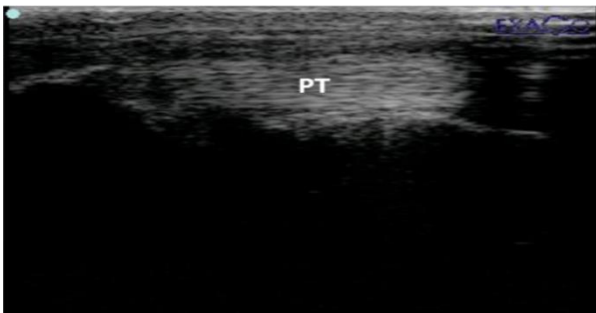


Fig. 8: Longitudinal scan at just close to lateral patellar ligament demonstrating flat echogenic structure representing the tendon of origin of peroneus tertius (PT) extending over the hyperechoic surface of the tibia.

DISCUSSION

The present study presented a detailed description of the ultrasonographic appearance of the stifle joint in clinically normal donkeys. Ultrasonography has the advantages of being noninvasive, fast, economic and convenient diagnostic tool allowing visualization of the articular and peri-articular structures (Adrian *et al.*, 2017; Martins *et al.*, 2006; Patil and Dasgupta, 2012; Penninck *et al.*, 1991). It overcomes the limitation of radiography (size of animal and type of equipment) and arthroscopy (invasiveness, requirement of general anesthesia and limited visualization of peri-articular structures) (Adrian *et al.*, 2017). All examinations were done in non-sedated standing position as the technique was well tolerated by all donkeys.

Many literatures have been published describing the ultrasonographic characteristics of the stifle joint in horses (Cauvin *et al.*, 1996; Coudry and Denoix, 2005; Denoix and Lacombe, 1996; Dik, 1995; Gottlieb *et al.*, 2016; Martins, Silva and Baccarin, 2006; Whitcomb, 2012) and we cannot rely on these data in donkeys due to anatomical and conformational variations (Burden and Thiemann, 2015).

In the present study, the systematic examination of the stifle region was based on the previously established palpable anatomical landmarks of horse (Cauvin, 2014; Whitcomb, 2012). This technique allowed obtaining standardized, consistent and repeatable images of the stifle region.

In supra-patellar approach, the anechoic supra-patellar pouch was the ultrasonographic land mark for the supra-patellar region where the thick curved echogenic

proximal border of the patella and the characteristic hypoechoic muscular pattern of the quadriceps muscle could be efficiently visualized and differentiated.

The proper visualization of the FP joint through supra-patellar approach during full weight bearing could be attributed to the cranio-dorsal position of the patella during full weight bearing which allowed wider supra patellar scanning zone. Moreover, most of the femoral trochlea is hidden by the patella when the stifle is flexed (Cauvin, 2014).

Superior imaging of the FT joint through cranial transverse scanning was attributed to the semi-flexed nature of the stifle joint, superficial location of joint compartments as well as the abundance of musculature at the caudal aspect. The elevated outer border of the menisci (Sisson and Grossman, 1975) hindered the feasibility of joint imaging from medial and lateral approaches while, the concave cranial surface provided a wide acoustic window. The medial compartment of the FT joint was ultrasonographically wider than the lateral compartment which is compatible with the anatomical feature of the joint (Sisson and Grossman, 1975).

In horses, the longitudinal scan was more superior to the transverse scan in visualizing the FT joint (Whitcomb, 2008) while in the present study, both transverse and longitudinal scans allowed efficient visualization of the joint.

The joint capsule and the infra-patellar fat pad couldn't be ultrasonographically differentiated due to their similar echogenicity; although they differ anatomically and histologically (Cauvin *et al.*, 1996).

Imaging of the two patellar ligaments at the same transverse scan allowed ultrasonographic comparison of their echogenicity. The echogenic appearance of the MiPL compared with MPL and LPL reflects the compact and dense nature of this ligament. The faint anechoic lines in longitudinal scans and the anechoic dots in transverse scans within the vicinity of the patellar ligaments represent the division between fascicle bundles of the ligament that seen in some normal horses (Dyson, 2002).

The abaxial bulging of the LM was inconsistent finding in donkeys included in the current study while it was a consistent normal finding in horses (Cauvin, 2014, Whitcomb, 2012). The popliteal tendon was not visualized in all donkeys which could be attributed to its small size and its location between the LCL and the LM.

The main limitations of this study include the use of a relatively low number of clinically healthy donkeys and the absence of a parallel autopsy study. Further studies should be directed to the clinical application of ultrasonography in diagnosing donkeys with stifle joint disease.

On conclusion, ultrasonography allowed a detailed description of the articular and peri-articular structure of the stifle region in donkeys. Establishment of the normal ultrasonographic appearance of the stifle joint will be helpful in diagnosing donkeys with joint disease.

REFERENCES

- Adrian AM, Barrett MF, Werpy, NM *et al.*, 2017. Comparison of arthroscopy to ultrasonography for identification of pathology of the equine stifle. *Equine Vet J* 49: 314-321.

- Beccati F, Chalmers HJ, Dante S *et al.*, 2013. Diagnostic sensitivity and interobserver agreement of radiography and ultrasonography for detecting trochlear ridge osteochondrosis lesions in the equine stifle. *Vet Radiol Ultrasound* 54: 176-184.
- Beccati F, Gialletti R, Passamonti F *et al.*, 2015. Ultrasonographic findings in 38 horses with septic arthritis/tenosynovitis. *Vet Radiol Ultrasound* 56: 68-76.
- Burden F and Thiemann A 2015. Donkeys Are Different. *J Equine Vet Sci* 35: 376-382.
- Cauvin KE 2014. Ultrasonography of the stifle. pp. 161-181. In: *Atlas of equine ultrasonography*, 1st ed (Kidd JA, Lu KG and Frazer ML), John Wiley & Sons, Ltd.
- Cauvin KE, Munroe GA, Boyd JS *et al.*, 1996. Ultrasonographic examination of the femorotibial articulation in horses: imaging of the cranial and caudal aspects. *Equine Vet J* 28: 285-296.
- Coudry V and Denoix JM, 2005. Ultrasonography of the femorotibial collateral ligaments of the horse. *Equine Vet Educ* 17: 275-279.
- Denoix JM and Lacombe V, 1996. Ultrasound diagnosis of meniscal injuries in horses. *Pferdeheilkunde* 12: 629-631.
- Dik KJ, 1995. Ultrasonography of the equine stifle. *Equine Vet Educ* 7: 154-160.
- Dyson SJ, 2002. Lameness associated with the stifle and pelvic regions. *A.A.E.P. Proceeding* 48: 387-411.
- Gottlieb R, Whitcomb MB, Vaughan B *et al.*, 2016. Ultrasonographic appearance of normal and injured lateral patellar ligaments in the equine stifle. *Equine Vet J* 48: 299-306.
- Jeffcott LB and Kold SE, 1982. Stifle lameness in the horse: A survey of 86 referred cases. *Equine Vet J* 14: 31-9.
- Kofler J, 1999. Ultrasonographic examination of the stifle region in cattle- normal appearance. *Vet J* 158: 21-32.
- Macrae AI and Scott PR, 1999. The normal ultrasonographic appearance of ovine joints, and the uses of arthrosonography in the evaluation of chronic ovine joint disease. *Vet J* 158: 135-143.
- Martins EA, Silva LC and Baccarin RY, 2006. Ultrasonographic changes of the equine stifle following experimental medial patellar desmotomy. *Can Vet J* 47: 471-474.
- Nayseh K, Kramer M and Ondreka N, 2015. Ultrasonographic examination of the stifle joint in the dog. Part 1: ultrasonographic anatomy, standardized scanning protocol and common indications. *Tierarztl Prax Ausg K Kleintiere Heimtiere* 43: 120-129.
- Patil P and Dasgupta B, 2012. Role of diagnostic ultrasound in the assessment of musculoskeletal diseases. *Ther Adv Musculoskel Dis* 4: 341-55.
- Pearson RA and Owassat M, 2000. A guide to live weight estimation and body condition scoring of donkeys. Scotland: Centre for Tropical Veterinary Medicine, University of Edinburgh. Institut Agronomique et Veterinaire, Hassan II, Rabat, Morocco.
- Penninck DG, Nyland TG, O'Brien TR *et al.*, 1990. Ultrasonography of the equine stifle. *Vet Radiol* 31: 293-8.
- Reardon R and Lischer C, 2008. Diagnosis and management of acute stifle injury in adult horses. *In Pract* 30: 426-33.
- Sisson S and Grossman JD, 1975. Equine syndesmyology.p.p. 349-375. In: *The Anatomy of the Domestic Animals* 5th ed (Getty R.). Philadelphia, PA, WB Saunders.
- Sullins KE, 2011. The stifle. pp.783-813. In: *Adams' Lameness in Horses* 6th ed (Baxte, G.M.) Lippincott Williams & Wilkins, Philadelphia.
- Trencart P, Alexander K, De Lasalle J *et al.*, 2016. Radiographic evaluation of the width of the femorotibial joint space in horses. *Am J Vet Res* 77: 127-36.
- Whitcomb MB, 2008. Ultrasonography of the equine stifle. *Ameveq Ultrasound Seminar-Bogota, Colombia* June 19-21.
- Whitcomb MB, 2012. Ultrasound of the equine stifle: basic and advanced techniques. In: *Proceedings of the AAEP Focus on Hind limb Lameness*, Oklahoma City, Oklahoma, pp: 1-3.